24P

HYDROGEN AND FLUORINE IN THE SURFACES OF LUNAR SAMPLES*

D.A. Leich†, R.H. Goldberg, D.S. Burnett, and T.A. Tombrello

California Institute of Technology, Pasadena, California 91109

ABSTRACT

The resonant nuclear reaction $^{19}F(p,\alpha\gamma)^{16}O$ has been used to perform depth-sensitive analyses for both fluorine and hydrogen in lunar samples. The resonance at 0.83 MeV (center-of-mass) in this reaction has been applied to the measurement of the distribution of trapped solar protons in lunar samples to depths of $\sim 1/2$ μm. These results are interpreted in terms of terrestrial H_2O surface contamination and a redistribution of the implanted solar H which has been influenced by heavy radiation damage in the surface region. Results are also presented for an experiment to test the penetration of H_2O into laboratory glass samples which have been irradiated with ^{16}O to simulate the radiation damaged surfaces of lunar glasses. Fluorine determinations have been performed in a 1 μm surface layer on lunar samples using the same $^{19}F(p,\alpha\gamma)^{16}O$ resonance. The data are discussed from the standpoint of lunar fluorine and Teflon contamination.

*Supported in part by the National Science Foundation [GP-28027] and the National Aeronautics and Space Administration [NGR 05-002-333].

†Present address: Physics Department, University of California, Berkeley, California 94720.

ONE OF THE LIME AID PREPRINT SERIES
IN NUCLEAR GEOPHYSICS AND COSMOCHEMISTRY

April 1974

HYDROGEN AND FLUORINE IN THE SURFACES OF LUNAR SAMPLES*

D.A. Leich†, R.H. Goldberg, D.S. Burnett, and T.A. Tombrello

California Institute of Technology, Pasadena, California 91109

ABSTRACT

The resonant nuclear reaction $^{19}F(p,\alpha\gamma)^{16}O$ has been used to perform depth-sensitive analyses for both fluorine and hydrogen in lunar samples. The resonance at 0.83 MeV (center-of-mass) in this reaction has been applied to the measurement of the distribution of trapped solar protons in lunar samples to depths of $\sim 1/2$ μm. These results are interpreted in terms of terrestrial H_2O surface contamination and a redistribution of the implanted solar H which has been influenced by heavy radiation damage in the surface region. Results are also presented for an experiment to test the penetration of H_2O into laboratory glass samples which have been irradiated with ^{16}O to simulate the radiation damaged surfaces of lunar glasses. Fluorine determinations have been performed in a 1 μm surface layer on lunar samples using the same $^{19}F(p,\alpha\gamma)^{16}O$ resonance. The data are discussed from the standpoint of lunar fluorine and Teflon contamination.

---

*Supported in part by the National Science Foundation [GP-28027] and the National Aeronautics and Space Administration [NGR 05-002-333].

†Present address: Physics Department, University of California, Berkeley, California 94720.

ONE OF THE LIME AID PREPRINT SERIES
IN NUCLEAR GEOPHYSICS AND COSMOCHEMISTRY

April 1974

I. Introduction

Solar wind ion implantation has been shown to be an important source of both high rare gas contents (see, for example, Eberhardt et al. 1970) and extreme radiation damage (Borg et al. 1971) within one micron of the surfaces of lunar soil grains. Significant surface-correlated enrichments of H, C, and N in lunar soils, due to solar wind implantation, have also been proposed (see, for example, Wszolek et al. 1974). Also, chemical and physical alterations of grain surfaces can be caused by solar wind related processes, including atmospheric reimplantation and ion sputtering, as well as unrelated mechanisms such as diffusive loss at lunar daytime temperatures, impact volatilization, condensation of impact-generated volatiles, and possibly, reaction with volcanic emanations.

In our continuing study, we have used a nuclear technique to investigate the effects of this complex environment on the depth distribution of hydrogen and fluorine in the outer micron of 2-5 mm lunar soil fragments and in chips from lunar rocks. Observed surface concentrations of hydrogen can be interpreted in terms of an expected solar wind source; however, the solar wind is not likely to be responsible for appreciable surface concentrations of fluorine. Consequently, measurements of the fluorine distributions in the outer micron of lunar sample surfaces may yield information concerning other processes such as the mobilizations of volatiles on the moon or reaction of the sample surfaces with fluorine-bearing volcanic emanations (Turkevich 1973).

II. Experimental Technique

The basic technique has been described in detail elsewhere (Leich and

Tombrello 1973), but a few points bear repeating. Both hydrogen and fluorine measurements are performed using the narrow (5 keV wide) resonance at 0.83 MeV center-of-mass energy in the nuclear reaction $^{19}F(p,\alpha\gamma)^{16}O$. A proton beam is directed onto the lunar sample for analysis of the fluorine distribution. Due to the sharp resonant nature of this reaction, the gamma-ray counting rate is proportional to the fluorine content at a particular depth determined by the choice of the incident proton energy. Higher energy protons penetrate deeper before being slowed down to the resonant energy. An analogous situation holds for measurement of the hydrogen distributions, in which a ^{19}F beam is used to induce the reaction on the hydrogen contained in the lunar sample. In either case, the gamma-ray counting rate is measured at a number of incident beam energies in the vicinity of the resonance, and these data are converted directly into a depth profile using proportionalities between beam energy and depth and between counting rate and concentration of hydrogen or fluorine. Measurements have been performed over the depth range for which this simple picture is valid; 0-0.5 μm for hydrogen, with a depth resolution of ~ 0.02 μm, and 0-1.0 μm for fluorine, with a resolution of ~ 0.05 μm.

A new scattering chamber has been used for some of the measurements reported in this paper, enabling the following improvements over the previous configuration described by Leich and Tombrello (1973).

A) The base pressure of the scattering chamber has been lowered from ~ 1×10^{-9} torr to $\lesssim 1 \times 10^{-10}$ torr.

B) The gamma-ray detection efficiency has been increased from ~ 0.02 to ~ 0.06.

C) Precise visual positioning of the beam on the target surface is now possible. Many samples fluoresce under bombardment, making the positioning quite accurate.

The following points should also be emphasized:

1) Both all metal scattering chambers have been vacuum baked and are pumped by clean, getter-ion pumps with a liquid nitrogen cooled baffle at the interface with the accelerator vacuum (~ 10^{-6} torr) to keep contamination to an absolute minimum. We have never seen a hydrogen buildup on any sample. Such buildup commonly occurs in poor vacuum as a result of beam-induced polymerization of residual hydrocarbon gases from the vacuum system.

2) We have observed no indication that exposure of lunar samples to atmospheric humidity affects the hydrogen contents of the samples below ~ 500 Å. Nevertheless, many of the samples used in this study have been carefully protected from atmospheric exposure by storing and handling them entirely in dry nitrogen gas following their return from the lunar surface in a vacuum-sealed sample container.

3) No attempt has been made to neutralize the charging of the sample due to bombardment of targets by the proton or $^{19}F^{4+}$ ion beams, other than to continuously collect the charge from the aluminum target holder. Surface potentials of 2-14 kV have been observed on these samples during illumination with the proton beam. A correction to the depth scale for the surface potential can be applied by measuring the apparent shift in the proton beam energy corresponding to an $^{27}Al(p,\gamma)^{28}Si$ resonance at 0.992 MeV proton energy (acting on the relatively uniform aluminum content of the lunar sample). While surface potentials of this magnitude are significant ($\lesssim$ 2000 Å) for the fluorine distribution data, potentials of a few tens of kilovolts have no significant effect on the hydrogen depth distribution measurements (Leich et al. 1973b).

4) We have never observed any indication that the hydrogen and fluorine implanted in the course of our analyses contribute to the measured concentrations. This observation is in agreement with the expected result based on the deep penetration of the energetic beam ions (~ 10 μm).

III. Hydrogen Depth Distributions

We have previously reported results of hydrogen profile measurements on a number of Apollo 11, Apollo 15, and Apollo 16 samples (Leich et al. 1973a and 1973b), noting that the hydrogen profiles measured on these samples fell into two distinct classes. One of these classes is characterized by a surface concentration of hydrogen, not more than a few hundred angstroms thick (e.g., the glass sphere profile in Fig. 1). The location of this hydrogen concentration appears to be reasonably consistent with expected solar wind proton penetration depths. However, small amounts of surface adsorbed hydrogen (~ 2×10^{15} atoms/cm^2, equivalent to one monolayer of H_2O) are routinely observed on interior rock samples which have been exposed only to dry nitrogen gas. The source of this adsorbed hydrogen is undoubtedly terrestrial (most likely the small residual H_2O content of the "dry" nitrogen), leading to the obvious conclusion that the similar features observed on the lunar exterior surfaces of the same samples, including sealed rock box samples, are due primarily to terrestrial contamination.

Figure 2 shows the results of a simulation experiment performed to determine the effects of extreme radiation damage on the adsorption and penetration of H_2O contamination. Fused silica targets were irradiated with 86 keV $^{16}O^+$ ions at doses up to 1.4×10^{17} ions/cm^2 in order to produce heavy

radiation damage down to depths of ~ 3000 Å. Subsequent exposure of some of these targets to water, in either liquid or vapor form, resulted in adsorption of measurable amounts of hydrogen surface contamination. Observed surface (within hundreds of angstroms) hydrogen concentrations were consistently a factor of two to three higher on the radiation damaged surfaces than on undamaged surfaces. However, the hydrogen concentrations exhibited only a slight dependence on the total dose between 2×10^{16} and 1.4×10^{17} ions/cm^2. Most importantly, it is evident from Fig. 2 that very little hydrogen contamination has penetrated to depths of 1000 Å or greater, in spite of the fact that radiation damage should be at saturation levels in the region from the surface to ~ 3000 Å deep (Winterbon et al. 1970). The similarity of the hydrogen profiles obtained on H_2O contaminated radiation damaged quartz glass samples with many of the lunar sample hydrogen profiles argues strongly for a similar origin of the observed hydrogen, namely terrestrial H_2O contamination preferentially bound on radiation damaged surfaces.

In addition to the surface adsorbed hydrogen, a small hydrogen content with a uniform distribution between ~ 1000 Å and 4000 Å deep (the limit of our measurements) has been observed in most of the interior rock samples, suggesting that this hydrogen component (normally between 20 and 50 ppm) is probably representative of a small volume content of lunar hydrogen in these rocks. An alternative explanation is that the deep hydrogen corresponds to H adsorbed on reentrant surfaces or along microfractures.

A second type of profile is characterized by an additional component with a maximum hydrogen content near 1000 Å deep and concentrated mainly within ~ 2000 Å of the surface (the full width at half maximum ranges from 1800 to 2700 Å with a mean of 2200 Å) and extending to depths greater than 4000 Å. Figures 1 and 3 show two examples of this type of distribution.

While extensive penetration of a terrestrial contaminant cannot be completely ruled out as possible origin for this hydrogen component, we believe we are measuring solar hydrogen because: (1) Exposure of artificially radiation-damaged fused silica surfaces to H_2O, even in liquid form, produced no penetration of H_2O to depths greater than 1000 Å, even for surfaces which were heavily damaged with ^{16}O ions prior to H_2O exposure (Fig. 2). (2) It appears doubtful that the exterior surfaces of 68815 and 70019, which had never been exposed to the atmosphere, could have adsorbed such large quantities of H_2O while the exterior surfaces of other samples, such as 68124,3 (the glass sphere, Fig. 1), returned in the same sealed rock box as 68815, showed only small quantities of surface adsorbed hydrogen. Given the known tendency of glasses to hydrate, the 68124,3 glass sphere would have been expected to adsorb much more H_2O than the surface of a crystalline rock sample such as 68815. (3) The large amounts of hydrogen observed in these samples are much greater than those seen in the damaged, H_2O-exposed glasses.

Our measurements of Apollo 17 samples, which consist of surface chips from two very different rocks, show similar hydrogen depth profiles. Sample 70019,17, shown in Fig. 3, is a glass-coated soil breccia which has a maximum hydrogen content near 1000 Å deep, closely paralleling 68815,27. Samples 75075,2 and 75075,18 are from opposite sides of a heavily patinated basalt; both were exposed to the solar wind. Although 75075 is very different physically from other samples we have measured, the hydrogen depth profiles are similar to 68815 and 70019 (see Fig. 4). Both 75075 and 70019 are sealed rock box samples and thus have not been exposed to atmospheric H_2O contamination. The hydrogen content of the deeper regions (100-200 ppm) is typical of lunar soil samples and this would be consistent with a model of patina formation by welded deposition of nearby soil (as opposed to splattering of

a coating from the host rock itself – see Blanford et al. 1974). However, the similarity of the overall profile to that found on unpatinated rock surfaces is suggestive of a patina formed from material which had not been exposed to solar wind prior to deposition. In either case the similarity of the 75075 profiles to those observed on unpatinated rocks or glass samples is best interpreted as indicating that the patina on these two surfaces has been deposited in layers at least 0.4 μm thick. Alternatively, it is more difficult to rule out H_2O contamination as an origin for the 75075 hydrogen because our argument that contamination H_2O does not penetrate to depths $\gtrsim$ 1000 Å may not be valid for the porous patina surface. However, the low hydrogen concentrations observed for the interior, soil breccia surface of 70019, which is similar material, argues against the 75075 profiles being contamination.

We now wish to consider in more detail the origin of the solar hydrogen at depths between 500 Å and 4000 Å in rocks such as 68815 and 70019. Although implantation of solar wind protons is the most likely original source, the observed hydrogen profiles are significantly more penetrating than would be derived from the direct implantation of solar wind protons, in agreement with conclusions based on chemical etching experiments for implanted rare gases (Eberhardt et al. 1970, Kirsten et al. 1970, Hintenberger et al. 1970). If solar wind is the source of this hydrogen component, extensive modification by diffusion and trapping of hydrogen atoms is implied. If diffusion rates for hydrogen in terrestrial silicates (Brückner 1971) are applicable to the lunar samples, it appears that bulk volume diffusion would be too rapid to result in the observed profiles without some sort of trapping to slow down the diffusion process (Ducati et al. 1973). A hypothesis in which implanted solar wind hydrogen diffuses rapidly into (and out of) the samples

with a small remnant of the implanted dose being retained in radiation damage traps seems plausible. The radiation damage is evidently so heavy in the outer 500 Å that no isolated traps remain (Borg et al. 1971). Beneath this depth relatively intense radiation damage (but below saturation) may persist to a depth of ~ 2000 Å, corresponding closely with the range of He ions with velocities near those of frequent high velocity (up to 800 km/sec) solar wind streams observed by satellites (Wolfe 1972). The population of isolated radiation damage traps by diffusing solar wind atoms may then result in a hydrogen depth profile which reflects the distribution of radiation damage. A discontinuity in the radiation damage gradient near 2000 Å deep may account for the characteristic bend observed in the measured hydrogen profiles, with the tail of the hydrogen distribution (below 2000 Å deep) representing diffusion of hydrogen out of the region of high hydrogen concentration into a region in which the radiation damage (due to solar flare and suprathermal ions) is much less intense. The slope of the hydrogen profile in the 2000 Å to 4000 Å depth region may reflect population of traps in a radiation damage gradient, or it may represent a dynamic profile of inward diffusion with weak trapping.

An alternative explanation for the observed hydrogen profiles is the direct implantation of "suprathermal" (10-100 keV) protons. If this hypothesis is correct, the measured hydrogen profiles provide information about the energy spectrum of the incident protons. A reasonably good fit to the initial set of hydrogen profile data for 68815,27 is shown by the solid curve in Fig. 5. This curve was obtained from range-energy relations (Lindhard et al. 1963) using the energy spectrum shown in Fig. 6, assuming that no post-implantation diffusion occurs and taking into account the effects of erosion and of incidence from a solar direction. A two component

energy spectrum is necessary to produce the characteristic bend in the profile near ~ 2000 Å deep. An atomic erosion rate of 0.5 Å/year and an erosional equilibrium profile has been assumed (Wehner et al. 1963), implying a long-term flux of suprathermal protons of ~ 10^{13} cm^{-2} y^{-1}, within a factor of about 3 of the flux for an event yielding the data shown in Fig. 6 taken from satellite observations (Frank 1970). Since the long-term flux of protons in this energy range is likely to be a few orders of magnitude lower than the flux during such an event, it appears unlikely that the average flux has been high enough to account for the measured hydrogen profiles by direct implantation. However, little data has been obtained in this energy range, and it is possible that long-term fluxes may have been high enough to account for a significant portion of the hydrogen distributions, or at least to account for a significant radiation damage gradient in the 2000 Å to 4000 Å depth region.

However, if the suprathermal hypothesis is adopted, it is still necessary to invoke radiation damage hindrance to explain why the direct implantation profile has not been modified by diffusion. The profile may or may not be controlled by the radiation damage gradient, depending on the strength of the trapping, and postulating a suprathermal flux may be unnecessary. In any case, the important point is that radiation damage is the dominant mechanism for localizing hydrogen near the surfaces of lunar samples.

IV. Fluorine Depth Distribution

Previously, we have reported fluorine surface concentrations (up to 1000 ppm) on several Apollo 16 samples which were much larger than those of bulk analyses of rocks (< 50 ppm) or soils (50-100 ppm) as reported by

Jovanovic and Reed (1973). However, the high (~ 2500 ppm) surface fluorine concentration measured by the in-situ Surveyor VII analysis (Patterson et al. 1970) agree with our data — if taken at face value. The critical question, which we were unable to answer previously, was the level of fluorine contamination. This is of particular concern because fluorine-rich materials (Teflon, Freon, etc.) have been used extensively both in the mission and post-mission handling of lunar samples. Our recent work has indicated that fluorine contamination is present — making the study of lunar surface fluorine difficult.

There are two features of our data which are not easily explained by contamination: (1) High fluorine concentrations are observed even at depths of 1 μm; this is illustrated in Fig. 7 (bottom) — for the cases of 66044,8 and 75075,2. The former is a 5 mm crystalline anorthosite fragment which has the highest surface-averaged fluorine concentration we have measured. Our measurements of 75075,2 are on a heavily patinated surface which shows a fluorine content similar to that of 66044,8. On 66044,8, the fluorine concentrations are high on two surfaces, and, along with 75075,2, are uniform at depths from 0.2 to at least 1 μm. Table 1 indicates the range of fluorine contents in the depth intervals 0-0.5 μm and 0.5-1.0 μm for some of the samples we have studied. While these high levels persist to 1 μm, our experience in hydrogen depth studies has shown the hydrogen contamination is usually manifested as a surface film which is less than ~ 0.1 μm thick. (2) Fluorine concentrations are usually much higher on the lunar exterior surface of rock chips than on the interior surface. The samples studied to date were allocated primarily for the purpose of hydrogen studies; in order to provide a dry N_2 atmosphere and to protect against surface abrasion during shipping, the samples were sealed in Teflon bags, excepting our

Apollo 17 samples, which were wrapped in aluminum foil prior to bagging. The interior surfaces produced by chipping in Houston provide a control on fluorine contamination from the packaging process. However, all rocks returned on Apollo 15-17 were contained in fluorocarbon bags cleaned in Freon, which could provide additional fluorine contamination on lunar exterior surfaces.

In order to measure the contamination due to Teflon packaging, we cleaned and baked quartz glass discs and found, after this procedure, a fluorine level of < 20 ppm. Two of these discs were transported to the curatorial facility where they were heat sealed in Teflon bags in the same way as lunar samples. Subsequent measurements showed a surface fluorine peak (~ 200 ppm) which at a depth of 1 μm had not yet reached zero (< 20 ppm) concentration (Fig. 8). The discs which remained in our laboratory as controls had < 20 ppm, as before. Figure 8 shows that readily measurable amounts of fluorine were produced either by the heat sealing or by abrasion; however, the amounts are much lower (by a factor of 5-10) than on lunar exterior surfaces. Conceivably, the rough surface of a rock is much more susceptible to contamination than the discs. However, the lunar interior samples packaged in Teflon tend to show concentrations no higher than those found on the discs. It is also clear from Fig. 8 that contamination is present to depths as great as 1 μm, implying that the high fluorine at this depth in lunar samples (see point [1]) could also be contamination.

If the surface fluorine contents represent contamination from the mission packaging materials, it is somewhat surprising that the most contaminated sample should be a coarse-fine fragment, because 66044,8 was transported to earth as part of a soil sample and, statistically, should have been protected. To check that 66044,8 was not an anomolously fluorine-rich lunar rock it was cleaved in half in our laboratory and fluorine measured on the interior surface.

As shown in Fig. 7 (bottom), the average fluorine content at 0.5-1.0 μm is ≤ 40 ppm, consistent with bulk fluorine measurements (Jovanovic and Reed 1973).

Although the consistently higher fluorine on exterior relative to interior surfaces suggests a lunar origin for the surface fluorine, we have some experimental evidence that the original arguments against contamination may not be valid. It may be that no lunar sample is sufficiently uncontaminated for the purposes of our experiment and perhaps other surface property experiments (e.g., carbon) as well. The only possibility would be samples from surface indentations, e.g., vesicles, which have been protected from abrasion, and some SESC or core samples that have never been exposed to teflon. Assuming that all fluorine we have observed is due to teflon, the associated carbon contamination would be insignificant in most bulk carbon chemistry studies.

We have so far limited the discussion to the measurement of surface fluorine layers because of their possible connection with condensation or reaction processes. It is clear that the interpretation of these results is clouded by the possibility of Teflon contamination; however, the use of our technique to determine bulk fluorine content is not open to question (see Fig. 7, bottom and Fig. 8). For example, an interior surface of 70019 that was freshly exposed in our laboratory has not been contaminated. This is confirmed by the flat fluorine depth distribution and the absence of a large surface peak — see the top part of Fig. 7. The concentration observed (~ 200 ppm) is approximately a factor of two higher than that found in most Apollo 16 samples (Jovanovic and Reed 1973); thus, we conclude that the soil breccia part of 70019 is a fluorine-rich lunar sample.

V. Summary

A significant portion of the hydrogen contents of lunar samples appears to reside within a few thousand angstroms of the sample surfaces. Besides surface contamination, in quantities corresponding to a monolayer ($\sim 2 \times 10^{15}$ H atoms/cm^2) or so of H_2O, and perhaps a small (normally 20-50 ppm) volume content of lunar hydrogen, an additional component has been observed in several of the lunar samples analyzed in this and previous studies. Although apparently of solar origin, the distribution of this component over characteristic depths of 1000-3000 Å shows that a simple picture of direct solar wind implantation is not adequate. Instead, the observed hydrogen depth distributions appear to result from some combination of a redistribution of solar wind hydrogen by diffusion and trapping in radiation damage sites and the direct implantation of "suprathermal" (10-100 keV) protons.

Although we are convinced that solar hydrogen has been measured in at least four of our samples [10085,31-12 (Leich et al. 1973a), 68815, 75075, and 70019], we do not understand why only these four show high concentrations. The 10085 and 70019 samples are glasses but 8 other glass samples analyzed (both coarse fines and rock surface chips) show low concentrations (Leich 1973). The 75075 (a patinated rock surface) sample is unique. However, 5 other rock samples which should be comparable to 68815 show only small concentrations (Leich 1973). This variability is puzzling and suggests that the nature of the "trapping" mechanism we postulate may be quite complex in detail.

In contrast to hydrogen, the fluorine contents of lunar sample surfaces are not likely to be strongly influenced by solar particle implantation. On the other hand, if volcanic emanations are present on the lunar surface, they

may, by analogy with terrestrial volcanic emanations, contain significant quantities of fluorine and other halogens. Thus, detection of surface enrichments of fluorine in lunar samples could indicate the presence of such emanations from the lunar interior. While consistently higher fluorine concentrations have been found on the lunar exterior surfaces than on the interior surfaces of the samples analyzed in this study, it is now certain that significant fluorine contamination has been introduced in the course of sample return and processing, and the possibility that the exterior surfaces were merely more thoroughly contaminated than the interior surfaces cannot, at this time, be ruled out. Hence, although tempted, we are unable to defend a lunar origin of observed surface enrichments of fluorine with presently measured samples.

Table 1. Fluorine concentration data in lunar samples. The two regions listed are surface 0-0.5 μm deep, and 0.5-1.0 μm deep. The positions for surface peaks listed are uncorrected for surface potentials created due to target charging.

Sample	Surface-averaged F content (ppm)		Surface Peak	
	0-0.5 μm	0.5-1.0 μm	position (μm)	FWHM (μm)
65315,6	1000	480	0.10	0.17
65315,6 interior	100	50	0.12	0.30
*68124,3-A	410	50	0.13	0.13
*68124,3-B	850	120	0.12	0.13
*66044,8-A	820	540	0.10	0.04
*66044,8-B	1900	1400	0.03	0.08
*66044,8 interior	75	40	0.02	0.15
†70019,17	235	60	0.12	0.17
†70019,17 interior	180	130	0.06	—
†75075,2	975	550	0.00	0.16
†75075,18	330	150	0.00	0.10

* Sealed rock box sample

† Sealed rock box sample; not Teflon bagged.

References

Blanford G., McKay D., and Morrison D. (1974) Accretionary particles and microcraters (abstract). In Lunar Science—V, pp. 67-69. The Lunar Science Institute, Houston.

Borg J., Maurette M., Durrieu L., and Jouret C. (1971) Ultramicroscopic features in micron-sized lunar dust grains and cosmophysics. Proc. Second Lunar Sci. Conf., Geochim. Cosmochim. Acta, Suppl. 2, Vol. 3, pp. 2027-2040. Pergamon.

Brückner R. (1971) Properties and structure of vitreous silica. II. J. Non-Crystalline Solids 5, 177-216.

Ducati H., Kalbitzer S., Kiko J., Kirsten T., and Müller H. W. (1973) Rare gas diffusion studies in individual lunar soil particles and in artificially implanted glasses. The Moon 8, 210-227.

Eberhardt P., Geiss J., Graf H., Grögler N., Krähenbühl U., Schwaller H., Schwarzmuller J., and Stettler A. (1970) Trapped solar wind noble gases, exposure age and K/Ar-age in Apollo 11 lunar fine material. Proc. Apollo 11 Sci. Conf., Geochim. Cosmochim. Acta, Suppl. 1, Vol. 2, pp. 1037-1070. Pergamon.

Frank L. A. (1970) On the presence of low-energy protons ($5 \lesssim E \lesssim 50$ keV) in the interplanetary medium. J. Geophys. Res. 75, 707-716.

Hintenberger H., Weber H. W., Voshage H., Wänke H., Begemann F., and Wlotzka F. (1970) Concentrations and isotopic abundances of the rare gases, hydrogen and nitrogen in Apollo 11 lunar matter. Proc. Apollo 11 Lunar Sci. Conf., Geochim. Cosmochim. Acta, Suppl. 1, Vol. 2, pp. 1269-1282. Pergamon.

Jovanovic S. and Reed G. W. Jr. (1973) Trace element studies in Apollo 16 samples (abstract). In Lunar Science—IV, pp. 418-420. The Lunar Science Institute, Houston.

Kirsten T., Müller O., Steinbrunn F., and Zähringer J. (1970) Study of distribution and variations of rare gases in lunar material by a microprobe technique. Proc. Apollo 11 Lunar Sci. Conf., Geochim. Cosmochim. Acta, Suppl. 1, Vol. 2, pp. 1331-1343. Pergamon.

Leich D. A. (1973) Applications of a nuclear technique for depth-sensitive hydrogen analysis: trapped H in lunar samples and the hydration of terrestrial obsidian (thesis). Unpublished.

Leich D. A. and Tombrello T. A. (1973) A technique for measuring hydrogen concentration versus depth in solid samples. Nuclear Instruments and Methods 108, 67-71.

Leich D. A., Tombrello T. A., and Burnett D. S. (1973a) The depth distribution of hydrogen in lunar materials. Earth Planet. Sci. Lett. 19, 305-314.

Leich D. A., Tombrello T. A., and Burnett D. S. (1973b) The depth distribution of hydrogen and fluorine in lunar samples. Proc. Fourth Lunar Sci. Conf., Geochim. Cosmochim. Acta, Suppl. 4, Vol. 2, pp. 1597-1612. Pergamon.

Lindhard J., Scharff M., and Schiøtt H. E. (1963) Range concepts and heavy ion ranges (notes on atomic collisions, II). Mat. Fys. Medd. Dan. Videnskab. Selskab 33, no. 14, 1-42.

Patterson J. H., Turkevich A. L., Franzgrote E. J., Economou T. E., and Sowinski K. P. (1970) Chemical composition of the lunar surface in a terra region near the crater Tycho. Science 168, 825-828.

Turkevich A. L. (1973) Private communication.

Wehner G. K., Kenknight C., and Rosenberg D. L. (1963) Sputtering rates under solar-wind bombardment. Planet. Space Sci. 11, 885-895.

Winterbon K. B., Sigmund P., and Sanders J. B. (1970) Spatial distribution of energy deposited by atomic particles in elastic collisions. Mat. Fys. Dan. Videnskab. Selskab 37, no. 14, 1-73.

Wolfe J. H. (1972) The large scale structure of the solar wind. Solar Wind, NASA SP-308, 170-196.

Wszolek P. D., O'Conner J. T., Walls F. C., and Burlingame A. L. (1974) Thermal release profiles and the distribution of carbon and nitrogen among minerals and aggregate particles separated from lunar soil (abstract). In Lunar Science—V, pp. 857-859. The Lunar Science Institute, Houston.

Figure Captions

Figure 1. Hydrogen concentration versus depth for three samples: breccia chip 68815,27, surface glass 65315,6, and glass spherule 68124,3. Smooth curves shown for the surface glass and glass sphere samples are drawn through the data points. 68815,27 and 68124,3 are sealed rock box samples.

Figure 2. Fused silica simulation experiment results. Data shown are representative of a set of samples subjected first to radiation damage and H_2O exposure tests. Two of the samples were damaged by irradiating them with 86-keV $^{16}O^+$ ions for 4 hours to a total dose of 1.4×10^{17} ions/cm^2. One of these (solid circles) was subsequently exposed to H_2O in both liquid (submerged in distilled water for 24 hr) and vapor (laboratory atmosphere for one week) form, while the other (solid triangles) was exposed only to dry N_2 gas for 2 hr. A third sample (open circles) was not radiation damaged but was given the same H_2O exposure as the first sample. Only sample error bars are shown on the data points obtained during the subsequent H analysis, performed to determine the extent of H_2O penetration. The solid curve represents typical results for a clean fused silica sample with a normal (for this batch) H content of $\sim$ 20 ppm.

Figure 3. Hydrogen concentration versus depth for 70019,17, a glass coated soil breccia chip (sealed rock box sample). The exterior surface was glass; the interior surface, soil breccia. During bombardment the H is relatively mobile, as indicated by the difference in the first and second run.

Figure 4. Hydrogen concentration versus depth for two 75075 samples (from sealed rock box) 75075,2 and 75075,18, both patinated surface chips. The curve for 75075,2 is drawn through the data points.

Figure 5. Implantation of solar protons in lunar samples. The data points are from sample 68815,27 (Fig. 1). The solid curve is the distribution resulting from the flux spectrum indicated by the solid lines in Figure 6, assuming an atomic erosion rate of 0.5 Å/yr, and calculated from the expected flux, incidence angle, irradiation time, and projected range of suprathermal protons (Leich 1973). The spectrum was chosen to give a rough fit to the data, using a proton range-energy relation derived from Lindhard et al. (1963) and neglecting range straggling and diffusion. The dashed curve indicates the limit of penetration of the present-day solar wind, including the effects of range straggling. With no diffusive losses in 4×10^6 yr, the peak hydrogen content at the surface would be greater than 10^{23} H atoms/cm^3, more than two orders of magnitude higher than the observed hydrogen content near the surface of sample 68815,27.

Figure 6. "Suprathermal" proton flux spectrum $d\phi/dE$ versus proton energy E. Data points with associated error bars are taken from satellite observations reported by Frank (1970). A spectrum adjusted to give a rough fit to the observed hydrogen distribution in 68815,27, assuming an atomic erosion rate of 0.5 Å/yr, is indicated by the solid lines.

Figure 7. Top: Fluorine concentration versus depth for sample 70019,17 (sealed rock box sample). Exterior points are from measurements on the glass coating, interior points are from measurements of a freshly exposed soil breccia surface.
Bottom: Fluorine concentration versus depth for anorthosite coarse fine 66044,8, and patinated breccia 75075,2, both sealed rock box samples. Shown are data from two surfaces of 66044,8, and from an interior surface freshly exposed in our laboratory. The smoothed dashed curve is drawn through the data points of 75075,2.

Figure 8. Fluorine concentration versus depth for quartz glass discs: solid points correspond to one that was packaged in Teflon in the curatorial facility; open points to an identical disc that served as a control.

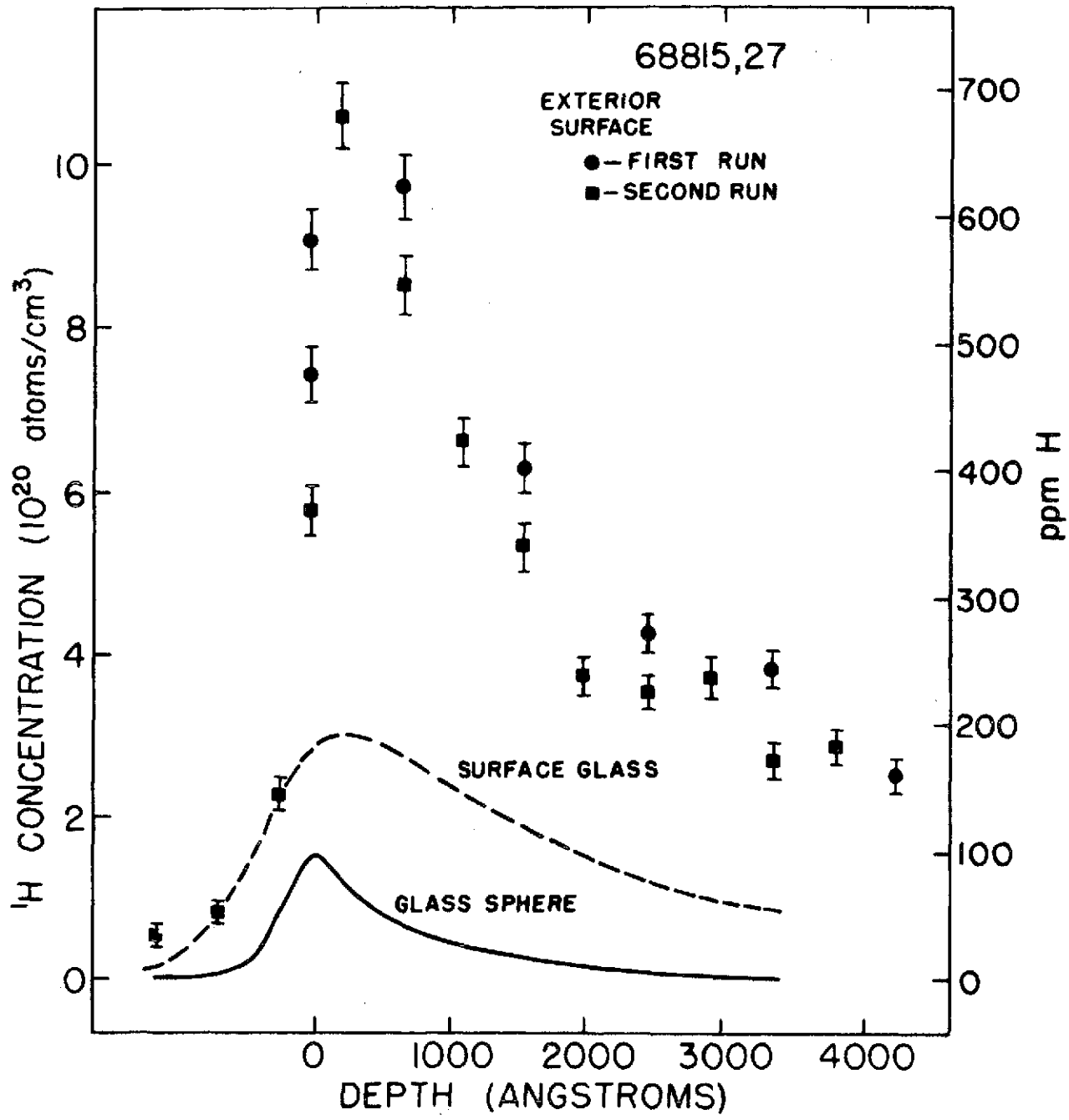
68815,27
EXTERIOR SURFACE
●—FIRST RUN
■—SECOND RUN
SURFACE GLASS
GLASS SPHERE
^{1}H CONCENTRATION (10^{20} atoms/cm^3)
ppm H
DEPTH (ANGSTROMS)
0
2
4
6
8
10
0
100
200
300
400
500
600
700
0
1000
2000
3000
4000

Fig. 1

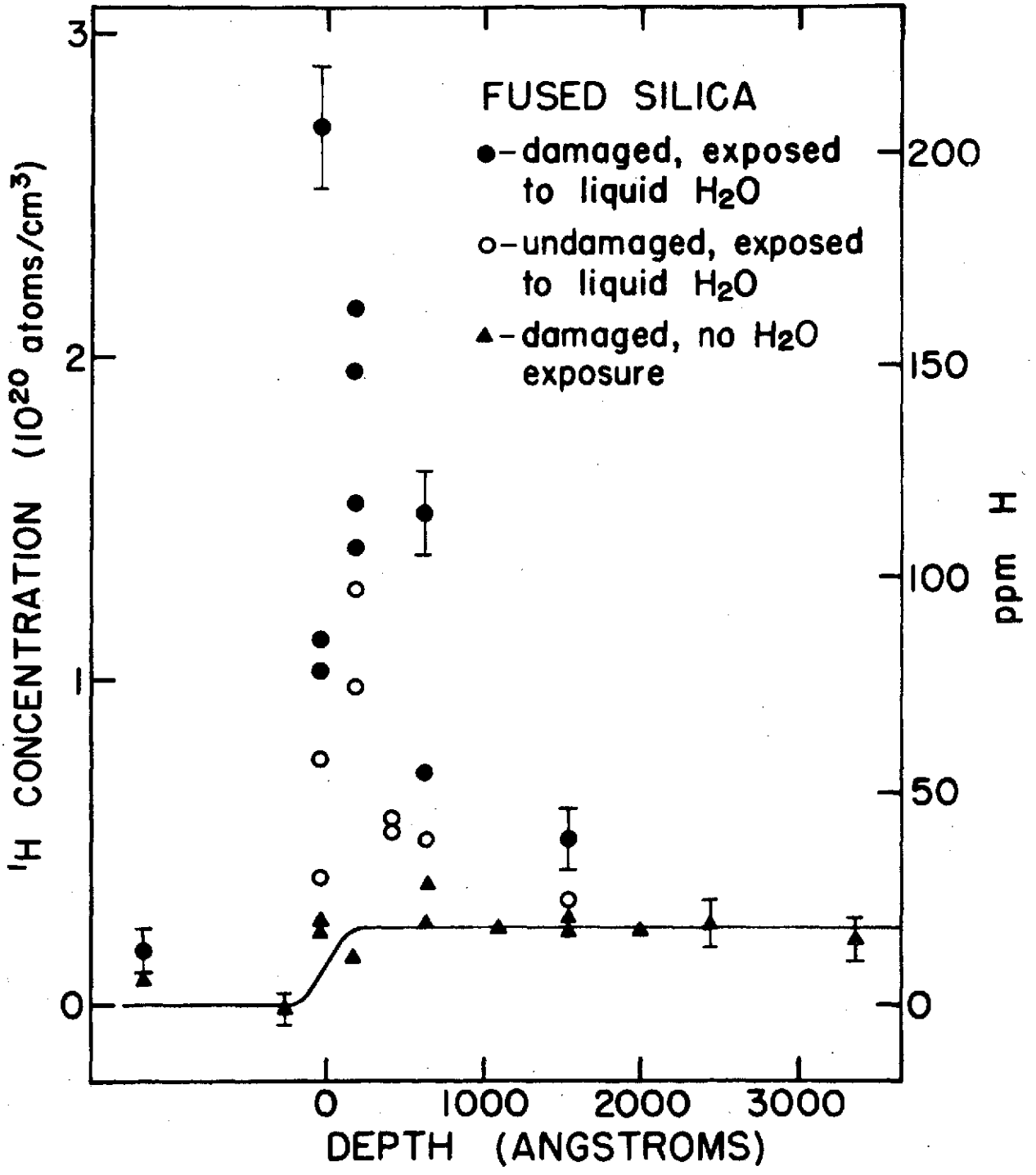
FUSED SILICA
●-damaged, exposed to liquid H_2O
○-undamaged, exposed to liquid H_2O
▲-damaged, no H_2O exposure
^1H CONCENTRATION (10^{20} atoms/cm^3)
ppm H
DEPTH (ANGSTROMS)
0
1
2
3
50
100
150
200
1000
2000
3000

Fig. 2

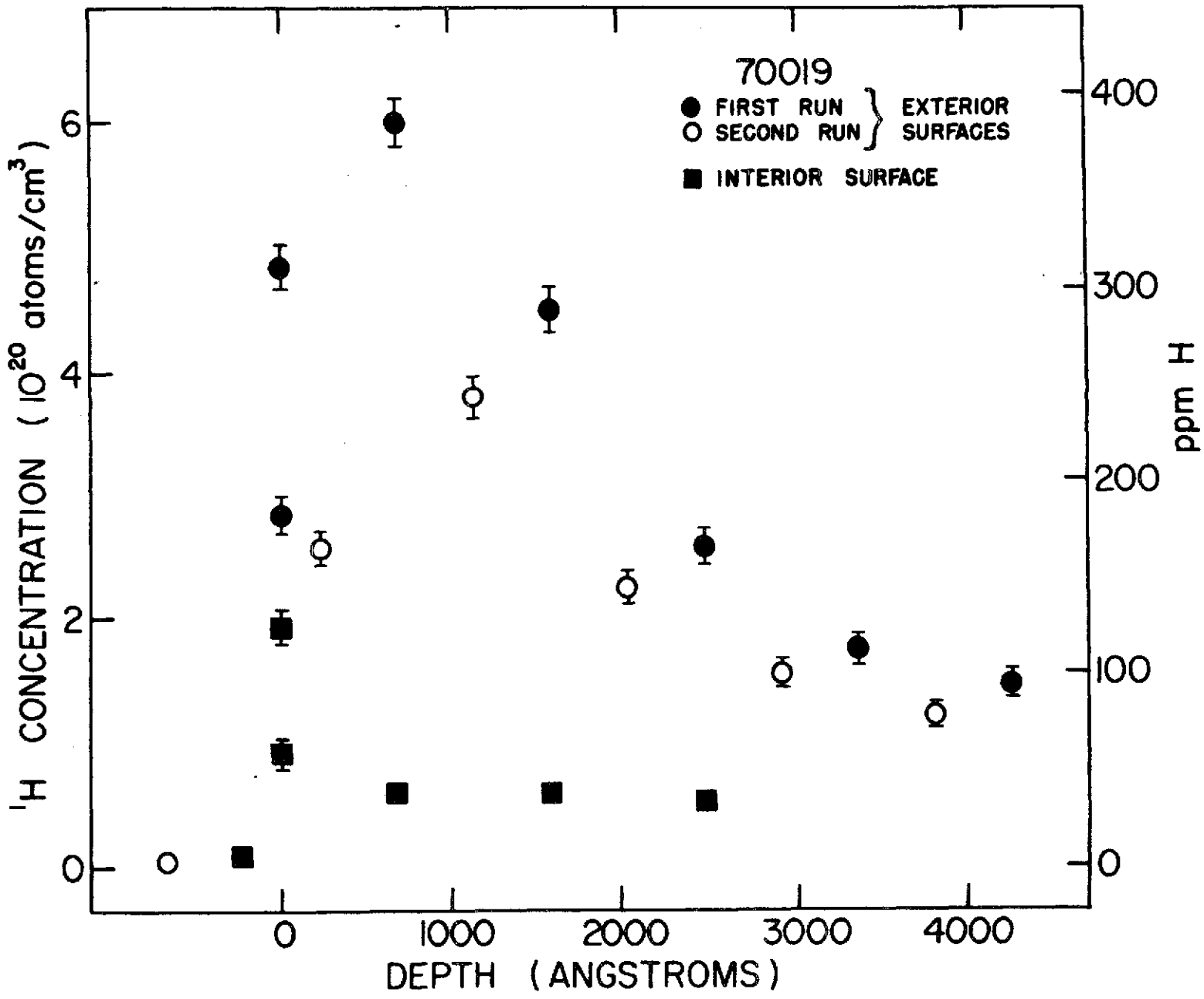
70019
FIRST RUN
SECOND RUN
EXTERIOR SURFACES
INTERIOR SURFACE
^{1}H CONCENTRATION (10^{20} atoms/cm^3)
ppm H
DEPTH (ANGSTROMS)
0
2
4
6
100
200
300
400
1000
2000
3000
4000

Fig. 3

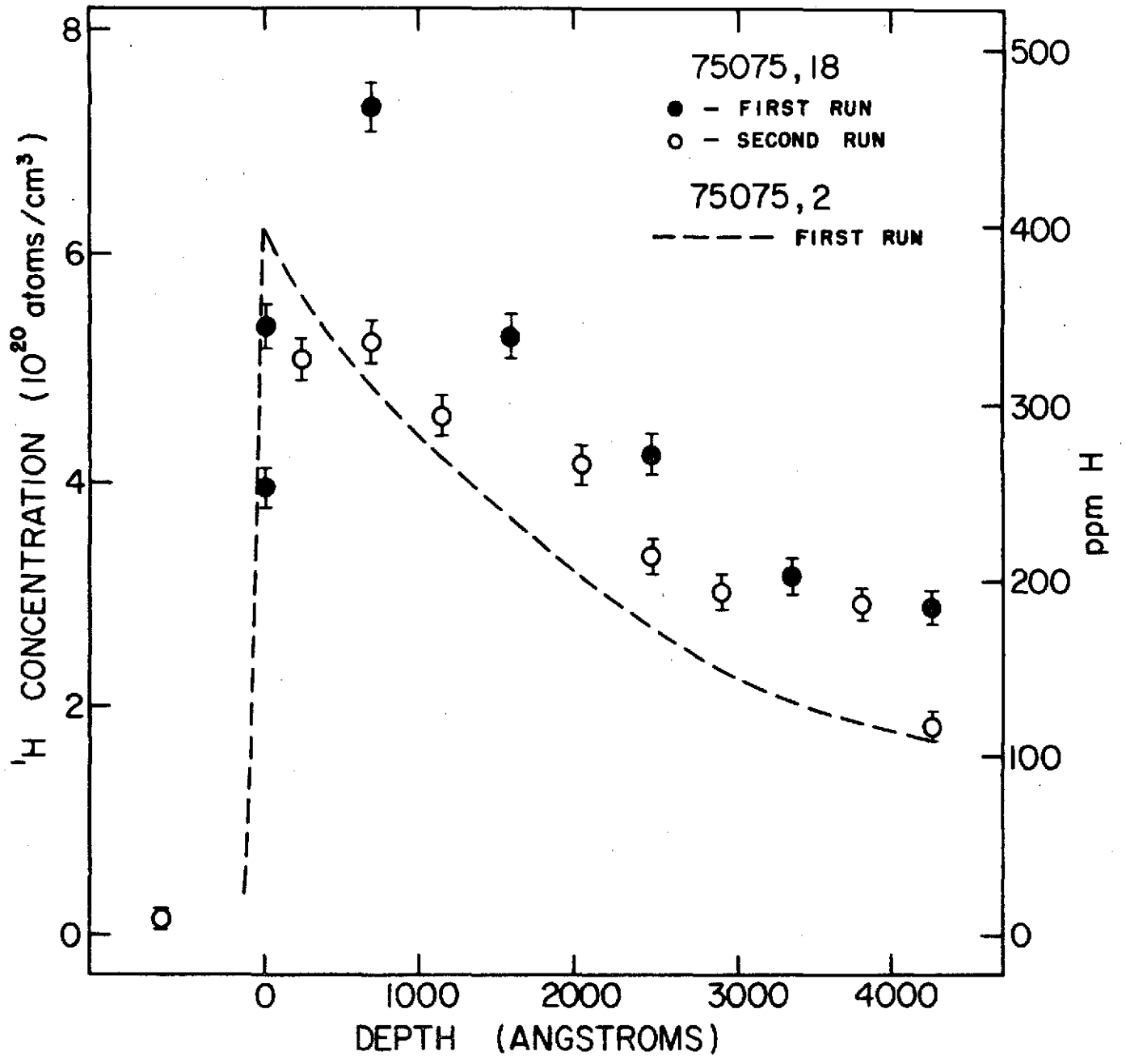
75075,18
● – FIRST RUN
o – SECOND RUN
75075,2
– – – – FIRST RUN
^{1}H CONCENTRATION (10^{20} atoms/cm^3)
ppm H
DEPTH (ANGSTROMS)
0
2
4
6
8
100
200
300
400
500
0
1000
2000
3000
4000

Fig. 1

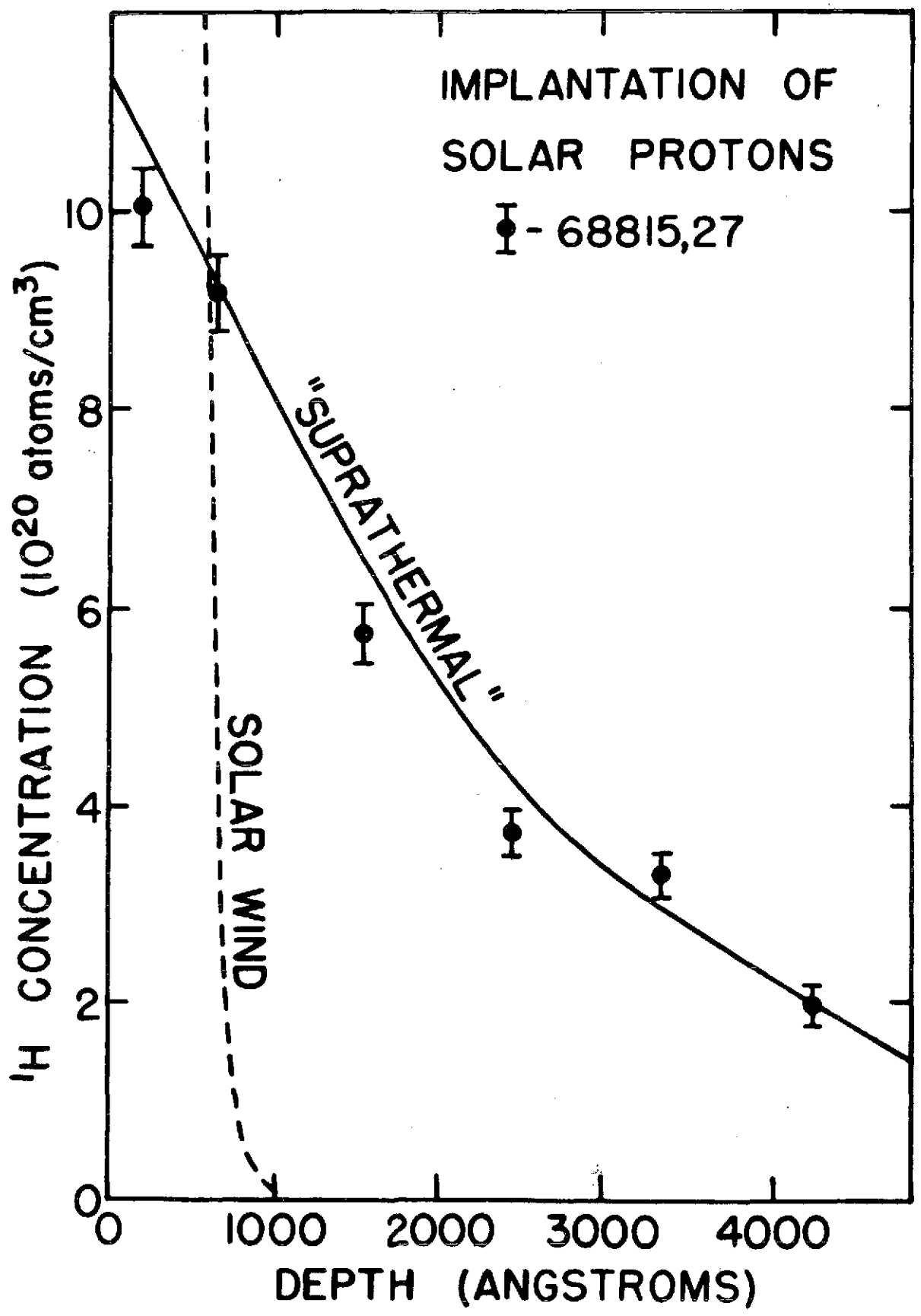
IMPLANTATION OF
SOLAR PROTONS
- 68815,27
"SUPRATHERMAL"
SOLAR WIND
^{1}H CONCENTRATION (10^{20} atoms/cm^3)
0
2
4
6
8
10
0
1000
2000
3000
4000
DEPTH (ANGSTROMS)

Fig. 5

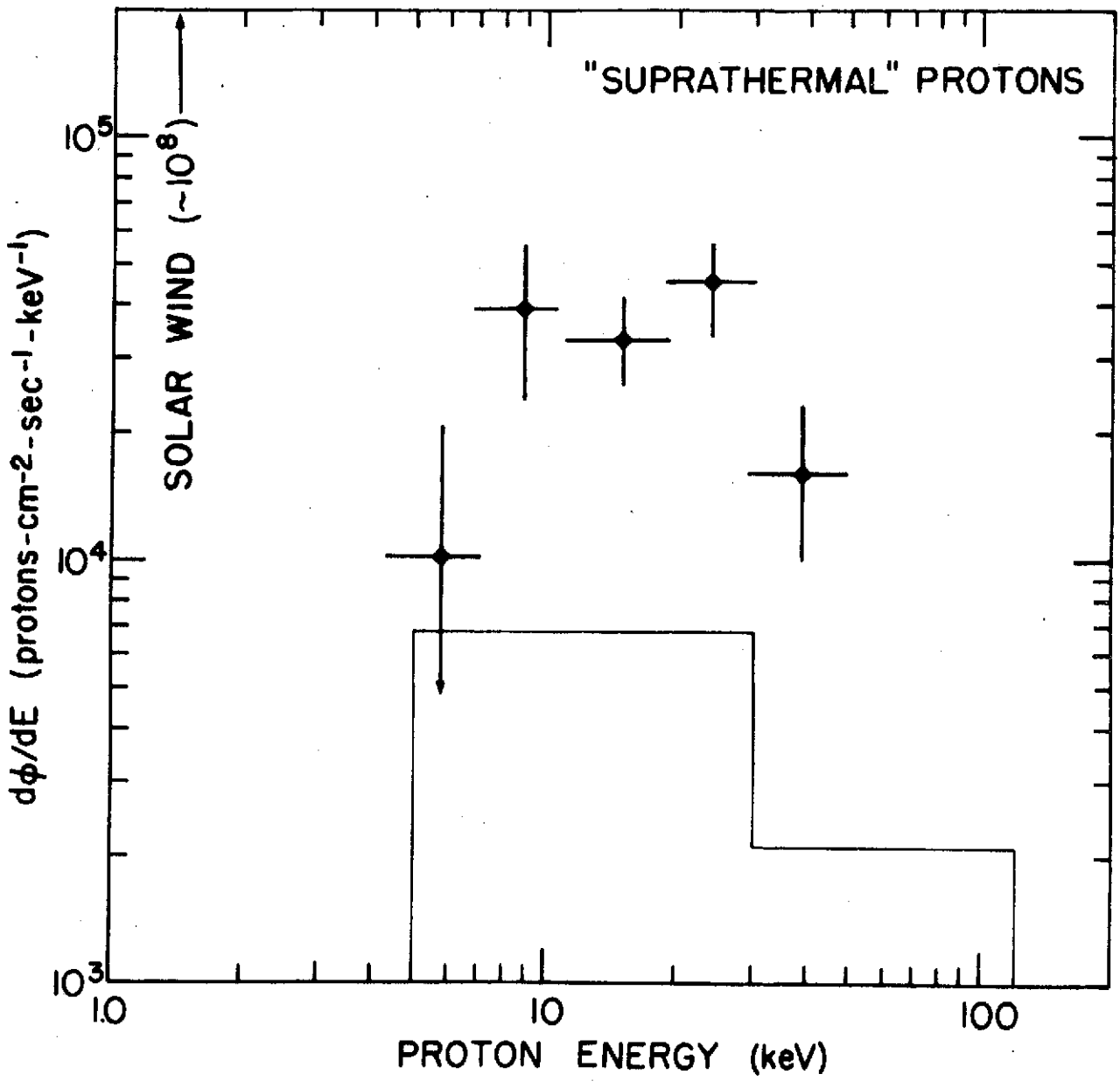
"SUPRATHERMAL" PROTONS
SOLAR WIND (~10^8)
dφ/dE (protons-cm^-2-sec^-1-keV^-1)
10^5
10^4
10^3
1.0
10
100
PROTON ENERGY (keV)

Fig. 6

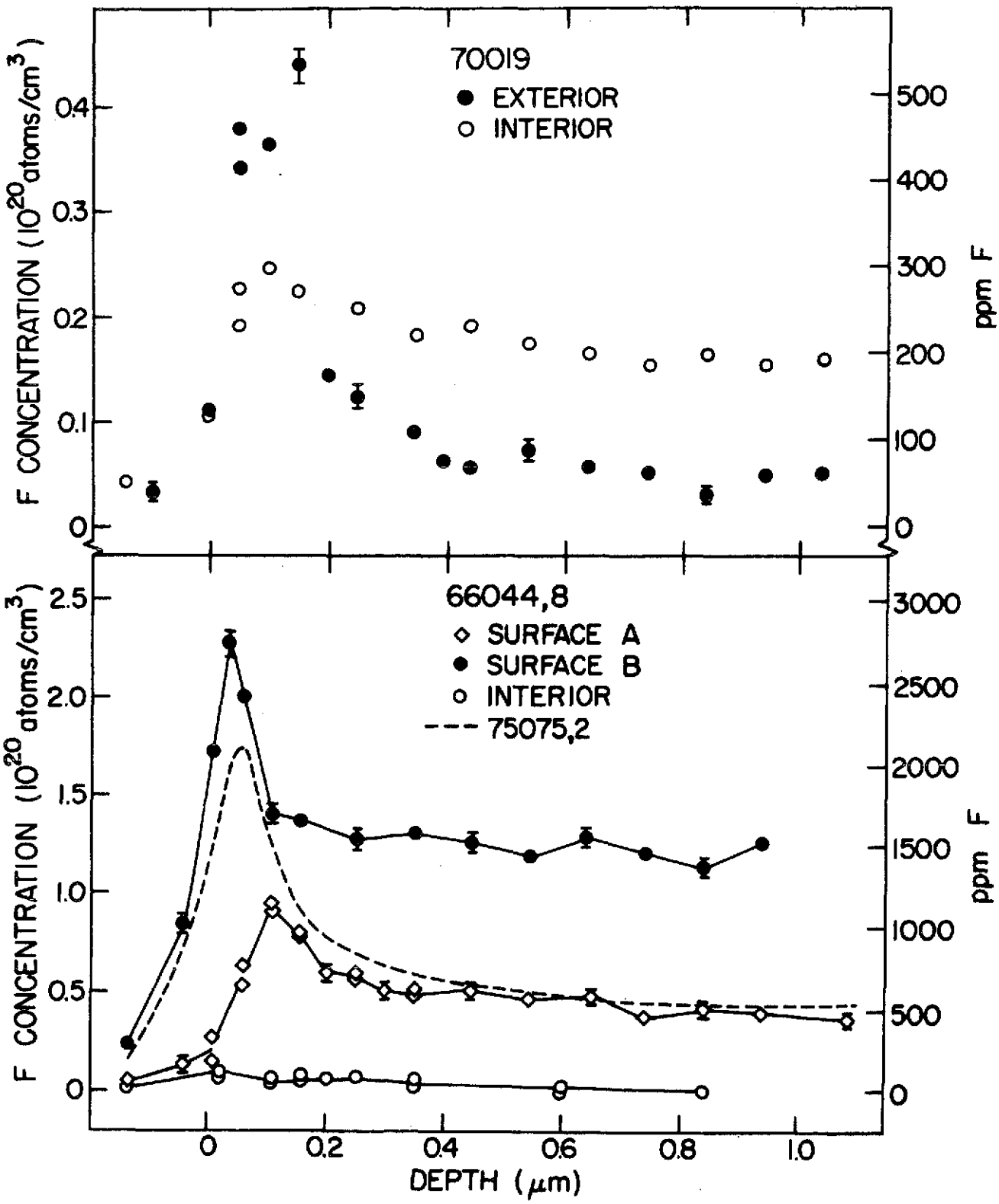
70019
EXTERIOR
INTERIOR
F CONCENTRATION (10^{20} atoms/cm^3)
ppm F
66044,8
SURFACE A
SURFACE B
INTERIOR
75075,2
DEPTH (μm)

Fig. 7

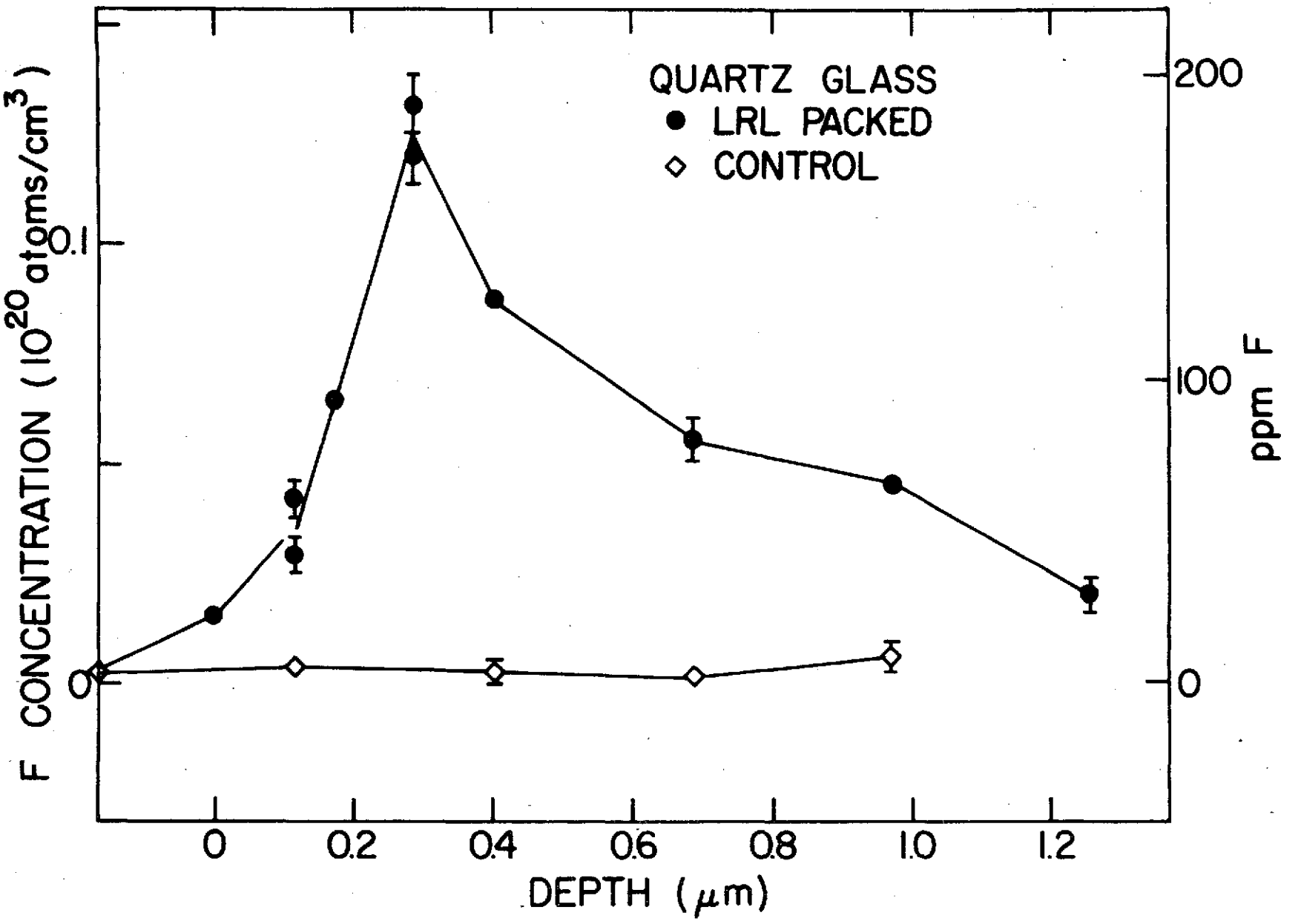
QUARTZ GLASS
LRL PACKED
CONTROL
F CONCENTRATION (10^{20} atoms/cm^3)
ppm F
DEPTH (μm)
0
0.1
200
100
0
0.2
0.4
0.6
0.8
1.0
1.2

Fig. 8